Interpretation of Activation Volumes for Water Exchange Reactions Revisited: *Ab Initio* Calculations for Al^{3+}, Ga^{3+}, and In^{3+}, and New Experimental Data

Th. Kowall,[†] P. Caravan,[†] H. Bourgeois,[†] L. Helm,[†] F. P. Rotzinger,*[,‡] and A. E. Merbach*[,†]

Contribution from the Institut de Chimie Minérale et Analytique, Université de Lausanne, Bâtiment de Chimie (BCH), CH-1015 Lausanne, Switzerland, and Institut de Chimie Physique, Ecole Polytechnique Fédérale Lausanne, CH-1015 Lausanne, Switzerland

Received February 19, 1998

Abstract: The water exchange mechanisms on the hexaaqua ions of Al^{3+}, Ga^{3+}, and In^{3+} in aqueous solution have been modeled by using ab initio calculations at the Hartree−Fock level. As an approximation aqua clusters in vacuo involving seven water molecules were considered. For species with five, six, or seven water molecules in the first coordination shell of the cation, stable intermediates and transition states have been optimized and characterized from vibrational analyses. Water exchange reaction pathways could then be proposed via interconnected intermediates and transition states. The calculations provide theoretical evidence for a break in kinetic behavior between Al^{3+} and Ga^{3+} on one side and In^{3+} on the other. Hexaaqua complexes of Al^{3+} and Ga^{3+} show no tendency to increase their coordination number over six and, despite the high positive charge on the central ion, water exchange proceeds via a D mechanism involving a pentacoordinated intermediate $[M(OH_2)_5 \cdot (OH_2)]^{3+}$. This is in agreement with experimental volumes of activation $\Delta V^{\ddagger}$ that are the highest measured up to date for trivalent metal cations. For $[In(OH_2)_6]^{3+}$ a dissociative exchange reaction is in principle feasible, but an associative A mechanism via a 7-fold coordinated reactive intermediate $[In(OH_2)_7]^{3+}$ is energetically much more favorable. Theoretical arguments and indirect experimental evidence in favor of an A and against an I_a mechanism are discussed. The experimentally still lacking activation volume $\Delta V^{\ddagger}$ for water exchange on $[In(OH_2)_6]^{3+}$ has been predicted to be -5 ± 1 cm^3mol^{-1}. The computed activation energies $\Delta E^{\ddagger}$ for Al^{3+} and Ga^{3+} are in remarkable quantitative agreement with the experimental values for $\Delta H^{\ddagger}$. This lends support to the applied theoretical model and suggests that for this class of aqua ions, with a spherical and strongly bound first hydration shell, cluster calculations in vacuo are a viable approach to reproduce the structural changes and the activation parameters for water exchange reactions in aqueous solution. Attempts have been made to determine the water exchange rate at $In^{3+}_{(aq)}$, $Lu^{3+}_{(aq)}$, and $Zn^{2+}_{(aq)}$ by using $Tb^{3+}_{(aq)}$ as a shift reagent. While none of these attempts proved successful, new lower limits for water exchange on these three ions can be given as 1×10^7 (In^{3+}), 1×10^7 (Lu^{3+}), and 5×10^7 s^{-1} (Zn^{2+}).

Introduction

The exchange reaction of a water molecule between the first hydration sphere and the bulk water

$$[M(H_2O)_n]^{z+} + nH_2O^* \rightleftarrows [\ddagger] \rightleftarrows [M(H_2O^*)_n]^{z+} + nH_2O \quad (1)$$

is fundamental to the understanding of the reactivity of metal ions in solution.

Experimentally, overall water exchange rates k can be determined from NMR kinetic measurements. The microscopic nature of the underlying reaction mechanism, however, is only indirectly accessible to experimental methods. In general, reaction mechanisms are suggested from experimentally testing the sensitivity of the reaction rate to a variety of chemical and physical parameters such as pressure, temperature, or concentration. Langford and Gray[1] classified substitution mechanisms into three categories: associative (A) where an intermediate of increased coordination number could be detected, dissociative (D) where an intermediate of reduced coordination number could be detected, and interchange (I) where there is no kinetically detectable intermediate. Operational tests such as the influence of the incoming group or the variation of the leaving group can allow the interchange mechanism to be described as **a** activated, I_a, or **d** activated, I_d.

For many metal ions the volume of activation $\Delta V^{\ddagger}$ linked to the water exchange reaction can be accurately determined from variable-pressure NMR kinetic experiments. $\Delta V^{\ddagger}$ can be interpreted as a measure of the degree of bond formation or bond breakage that occurs in the transformation to the transition state and constitutes very often the most decisive clue as to the microscopic nature of the substitution reaction and to the mechanistic classification.[2] Large positive or negative values of the activation volume $\Delta V^{\ddagger}$ are indicative for a pathway via a stable intermediate of either decreased or increased coordination number, i.e. a dissociative D or an associative A mechanism.

[†] Université de Lausanne.
[‡] Ecole Polytechnique Fédérale Lausanne.

(1) Langford, C. H.; Gray, H. B. *Ligand Substitution Dynamics*; Benjamin: New York, 1965.
(2) Swaddle, T. W. *Adv. Inorg. Bioinorg. Mech.* **1983**, *2*, 95.

S0002-7863(98)00571-X CCC: $15.00
Published on Web 06/19/1998

Smaller values of $\Delta V^{\ddagger}$ hint to concerted reactions via a transition state that may have some dissociative (I_d) or associative (I_a) character.

Today a large number of experimental results for the water exchange kinetics of most of the metal ions in aqueous solution have been accumulated and have revealed a wide spectrum of kinetic behavior.[3] Exchange rate constants measured to date extend over roughly 20 orders of magnitude between $[Ir(H_2O)_6]^{3+}$ (residence time of a particular coordinated water molecule $\tau_{res} = 300$ years[4]) and Cu^{2+} ($\tau_{res} = 227$ ps[5]). Observed activation volumes $\Delta V^{\ddagger}$ vary between -12.1 cm^3/mol for $[Ti(OH_2)_6]^{3+6}$ and $+7.2$ cm^3/mol for $[Ni(H_2O)_6]^{2+}$.[7] These experimental data are now spurring on theoretical calculations to see how well kinetic parameters can be reproduced and to test independently the assumptions made in mechanistic interpretations.

Classical molecular dynamics simulations (MD) where cations are immersed in several hundred water molecules provide the most direct approach for theoretically studying ion solvation and water exchange phenomena as they yield a complete molecular picture both of the water structure around the ion and of the water exchange reaction. Exchange rate constants can be ideally obtained from simply counting the number of exchange events. Moreover, MD simulations illustrate the fact that individual ligand exchange events at $T > 0$ K in a solvent may follow a distribution of reaction pathways. To reproduce macroscopic activation parameters, e.g. $\Delta H^{\ddagger}$ or $\Delta V^{\ddagger}$, MD simulations offer a means to efficiently sample all relevant microscopic exchange pathways and to average activation profiles from individual events. There have been reports of residence times τ_{res} extracted from MD simulations for the alkali metal ions.[8−10] Recently, a detailed picture of the structure and kinetics of aqueous solutions of lanthanide ions, Ln^{3+}, has been developed by means of MD simulations.[11] The hydration of this class of cations is an ideal case for classical MD simulation studies. First of all, even for the 3-fold charged lanthanide ions the exchange of coordinated water takes place in the subnanosecond regime and is therefore within the reach of today's computers. Moreover, the interaction between these "hard" metal ions and "hard" oxygen donor ligands such as water is nondirectional, without covalent contributions, and therefore well-represented by parametric Coulomb and van der Waals terms.

The hydration spheres of many cations outside the series of lanthanides or the alkali metals have considerable covalent character with transfer of electron density to the metal center and are often much less labile. Molecular dynamics simulations, which offer the advantage of realistically solvating metal ions and of taking explicitly into account the entropy term to $\Delta G^{\ddagger}$, are therefore not suitable for the less labile systems. Fortunately, when studying metal ions with a strongly bound first hydration shell and activation barriers for water exchange of several kT, quantum-mechanical studies of small metal−ion aqua clusters in vacuo at $T = 0$ K may be a viable alternative to MD simulations. For these aqua ions the energetics during a water exchange event are expected to be mainly determined by changes in the delicate balance between the strong water−ion attraction and the strong water−water repulsion inside the first hydration shell, with a much smaller perturbation from changes outside the first shell. Moreover, the structural disorder in the first hydration shell and the variability in the exchange pathways due to thermal motion is reduced, so that exploring the relevant part of the configuration space might be within the reach even of time-consuming quantum chemical calculations. Identifying chemically relevant stationary points and characterizing them in detail as intermediates or transition states then offers an elegant clue as to the nature of the exchange mechanism. Stable intermediates are clusters which possess no imaginary vibrational frequency, whereas transition states possess one and only one imaginary frequency.

Recently, Rotzinger has successfully applied a quantum chemical approach to the water exchange on the hexaaqua complexes of the first row transition metal ions, at first for Ti(III), V(II), and Ni(II)[12] as representative examples and later for the whole first transition series from Sc(III) to Zn(II).[13] After locating and optimizing relevant stationary points in the configuration space of aqua clusters of different coordination number, reaction pathways via interconnected intermediates and transition states have been proposed. This revealed how the most favorable exchange pathway is linked to the d-electron configuration of the cation and yielded structural changes during activation and activation energies $\Delta E^{\ddagger}$ in agreement with experimental $\Delta H^{\ddagger}/\Delta G^{\ddagger}$ and $\Delta V^{\ddagger}$ values. This agreement justifies the gas-phase model, neglecting changes in second sphere hydration energy during an exchange process. Further this study corrected at the same time earlier quantum chemical computations from Sandström and co-workers[14] that had cast doubt on the mechanistic assignments made on the basis of experimental values of activation volume for hexahydrated 3d metal ions. Water exchange has also been modeled on Pd(II) and Pt(II) aquaions by using density functional theory (DFT),[15] without, however, strictly characterizing the nature of the involved species from vibrational analysis. First results from DFT calculations on Zn^{2+}−aqua clusters have been reported by van Eldik and co-workers.[16]

The present article is meant to be the first step toward a thorough investigation of the hydration of the series of the trivalent cations Al^{3+}, Ga^{3+}, and In^{3+} in aqueous solution. Due to their closed shell configuration, they are favorable candidates for a rigorous quantum-mechanical study of their aqua clusters, applying the approach used previously.[12,13] Rate constants and activation parameters for water exchange on Al(III),[17] Ga(III),[18,19] and In(III)[20] have been determined from kinetic ^{17}O

(3) Lincoln, S. F.; Merbach, A. E. *Adv. Inorg. Chem.* **1995**, *42*, 1.
(4) Cusanelli, A.; Frey, U.; Richens, D. T.; Merbach, A. E. *J. Am. Chem. Soc.* **1996**, *118*, 5265.
(5) Powell, D. H.; Helm, L.; Merbach, A. E. *J. Chem. Phys.* **1991**, *95*, 9258.
(6) Hugi, A. D.; Helm, L.; Merbach, A. E. *Inorg. Chem.* **1987**, *26*, 4444.
(7) Ducommun, Y.; Newman, K. E.; Merbach, A. E. *Inorg. Chem.* **1980**, *19* 3696.
(8) Impey, P. W.; Madden, R. A.; McDonald, I. R. *J. Phys. Chem.* **1983**, *87*, 5071.
(9) Guàrdia, E.; Padró, J. A. *J. Phys. Chem.* **1990**, *94*, 6049.
(10) Lee, S. H.; Rasaiah, J. C. *J. Phys. Chem.* **1996**, *100*, 1420.
(11) (a) Kowall, Th.; Foglia, F.; Helm, L.; Merbach, A. E. *J. Am. Chem. Soc.* **1995**, *117*, 3790. (b) Kowall, Th.; Foglia, F.; Helm, L.; Merbach, A. E. *J. Phys. Chem.* **1995,** *99*, 13078. (c) Kowall, Th.; Foglia, F.; Helm, L.; Merbach, A. E. *Chem. Eur. J.* **1996**, *2*, 285.
(12) Rotzinger, F. P. *J. Am. Chem. Soc.* **1996**, *118*, 6760.
(13) Rotzinger, F. P. *J. Am. Chem. Soc.* **1997**, *119*, 5230.
(14) Åkesson, R.; Pettersson, L. G. M.; Sandström; M.; Wahlgren, U. *J. Am. Chem. Soc.* **1994**, *116*, 8705.
(15) Deeth, R. J.; Elding, L. I. *Inorg. Chem.* **1996**, *35*, 5019.
(16) Hartmann, M.; Clark, T.; van Eldik, R. *J. Mol. Model.* **1996**, *2*, 354.
(17) Hugi-Cleary, D.; Helm, L.; Merbach, A. E. *Helv. Chim. Acta* **1985**, *68*, 545.
(18) Fiat, D.; Connick, R. E. *J. Am. Chem. Soc.* **1968**, *90*, 608.
(19) Hugi-Cleary, D.; Helm, L.; Merbach, A. E. *J. Am. Chem. Soc.* **1987**, *109*, 4444.
(20) Glass, G. E.; Schwabacher, W. B.; Tobias, R. S. *Inorg. Chem.* **1968**, *7*, 2471.

NMR experiments. Due to the fast water exchange on In^{3+}, the NMR line broadening technique yielded only a lower limit for the exchange rate constant on hydrated In^{3+} and an experimental value for the activation volume $\Delta V^{\ddagger}$ is still lacking. Al^{3+} and Ga^{3+} possess the largest activation volumes $\Delta V^{\ddagger}$ that have been measured up to date for trivalent cations and are clearly exchanging via a dissociatively (**d**) activated mechanism, despite their high positive charge. Studies in nonaqueous solvents[3] suggest a D mechanism for Al^{3+} and Ga^{3+} crossing over to an **a** activation mode for In^{3+}. This is not surprising given that in the solid state there are many more In(III) complexes with a coordination number larger than six than there are Ga(III) complexes. It is one of the objectives of this study to see whether quantum mechanical calculations are capable of reproducing this break in kinetic behavior between Ga^{3+} and In^{3+} in water.

We have recently employed a terbium shift-reagent approach to determine the water exchange rate at the Mg^{2+} aqua ion ($k_{298} = 6.7 \times 10^5\ s^{-1}$).[21] This method should allow the determination of water exchange rates up to $10^7\ s^{-1}$ for diamagnetic species. Glass et al.[20] have given a lower limit on In^{3+} water exchange of $\geq 4 \times 10^4\ s^{-1}$. Employing the same approach as with Mg^{2+}, we hope to be able to determine the kinetic parameters k_{298}, $\Delta H^{\ddagger}$, $\Delta S^{\ddagger}$, and $\Delta V^{\ddagger}$ for In^{3+}.

Experimental Section

Terbium oxide (Alfa, 99.99%), indium perchlorate hydrate (Alfa), lutetium oxide (NuCor, 99.99%), zinc oxide (Alfa, 99.999%), 70% perchloric acid (Merck, p.a.), and ^{17}O enriched water (10 atom %, Yeda) were used as received. Terbium, lutetium, and zinc perchlorates were prepared as described previously.[22] Stock solutions of metal perchlorates were standardized by EDTA titration for metal content and by NaOH titration with use of Gran's method[23] to determine acid content. The indium and zinc salts were checked by ICP-AES for possible Mn(II) impurities, while the lutetium and terbium salts were checked by X-band EPR for possible Mn(II) impurity. All salts used contained less than 0.5 ppm Mn(II) in the solid.[24] ^{17}O enriched nitromethane[25] was used as an internal reference for chemical shift measurements. Solutions were prepared by weight (concentrations given as mole of metal ion per kilogram of solvent) and ranged from 0.3 to 0.5 *m* Tb^{3+}, 1−2 *m* Zn^{2+}, 0.3−3 *m* In^{3+} and Lu^{3+}, and 0.2 *m* $HClO_4$.

Variable-temperature ^{17}O NMR spectra were obtained with a Bruker AMX-600 operating at 81.3 MHz, using a 10 mm broad band probe and working without lock. Samples were sealed in spherical cells to minimize magnetic susceptibility effects.[26] Temperature was measured by a substitution technique.[27] Chemical shifts were measured relative to acidified water by fitting the resonances to Lorentzian line shape functions; in all instances an internal reference of ^{17}O enriched CH_3NO_2 (~0.02 *m*) was used. Longitudinal relaxation rates, $1/T_1$, were measured by the inversion−recovery method[28] and transverse relaxation rates, $1/T_2$, were measured by the Carr−Purcell−Meiboom−Gill spin−echo technique.[29]

Computational Methods

The *ab inito* calculations have been carried out at the restricted Hartree−Fock (SCF) level with use of the GAMESS program[30] on Silicon Graphics R8000 and HP 9000/735 workstations.

For the aluminum atom, the basis sets of Stevens, Basch, and Krauss[31] were used, for Ga and In basis sets of Stevens, Basch, Krauss, and Jasien[32] were taken, where for Ga and In the effective core potentials contain relativistic corrections. For Ga^{3+} the remaining 3s, 3p, 4s, and 4p shells have double-ζ and the 3d shell triple-ζ quality. For In^{3+} the remaining 4s, 4p, 5s, and 5p shells have double-ζ and the 4d shell triple-ζ quality. In the case of Al the basis set has been extended by an additional d function ($\alpha_{3d} = 0.30$).[33] For O and H 6-31G(d) basis sets[34] were used ($\alpha_{3d} = 1.20$).[33,12] For complexes the MP2 optimization of the Gaussian 94 package[35] was used.

The DFT calculations have been performed with the ADF 2.0.1 package (Department of Theoretical Chemistry, Vrije Universiteit, Amsterdam)[36] with use of basis sets IV/In.4p, IV/O.1s, and IV/H (they are of approximately triple-ζ quality with an additional polarization function). The local exchange-correlation functional of Vosko−Wilk−Nusair[37] and nonlocal corrections to the exchange and the correlation of Perdew and Wang,[38] respectively, were used. For In, scalar (quasi-) relativistic corrections[39] have also been applied.

The volumes of the clusters were calculated from solvent excluding surfaces (Connolly surfaces) by using the Cerius^2 package.[40] They were calculated with a probe radius of 1.40 Å and a dot density of 100 $Å^{-2}$ and by neglecting the volume of the hydrogen atoms.

Results

Reliability of the Calculations. The M−O bond lengths of the isolated hexahydrates $M(OH_2)_6^{n+}$ are known to be longer than those observed in crystals.[41] This arises from the omission of the second coordination sphere, the anions, and bulk water.[12,13] The structures of Al^{3+} and Ga^{3+} aqua complexes are expected to be as accurate as those involving first row transition metals, but for the complexes of the much heavier In^{3+} ion, the role of dynamic electron correlation and relativistic effects has to be analyzed. Hence, the structures of the $M(OH_2)_6^{3+}$ ions (M = Al, Ga, and In) have been optimized at the Hartree−Fock (neglecting dynamic electron correlation and

(21) Bleuzen, A.; Pittet, P.-A.; Helm, L.; Merbach, A. E. *Magn. Reson. Chem.* **1997**, *35*, 765.
(22) Cossy, C.; Helm, L.; Merbach, A. E. *Inorg. Chem.* **1988**, *27*, 1973.
(23) Gran, G. *Acta Chem. Scand.* **1950**, *4*, 559.
(24) Because of its potent ability as a T_2 relaxation agent for $H_2{}^{17}O$, and the fact that this study employed high concentrations of metal ions, it was found that concentrations of Mn(II) greater than 1 ppm in the metal salts used could lead to anomalous results.
(25) Sandler, S. R.; Karo, W. *Org. Func. Group Prepr.* **1968**, *1*, 425.
(26) Hugi, A. D.; Helm, L.; Merbach, A. E. *Helv. Chim. Acta* **1985**, *68*, 508.
(27) Amman, C.; Meyer, P.; Merbach, A. E. *J. Magn. Reson.* **1982**, *46*, 319.
(28) Vold, R. S.; Waugh, J. S.; Klein, M. P.; Phelps, D. E. *J. Chem. Phys.* **1968**, *48*, 3831.
(29) Meiboom S.; Gill, D. *Rev. Sci. Instrum.* **1958**, *29*, 688.
(30) Schmidt, M. W.; Baldridge, K. K.; Boatz, J. A.; Elbert, S. T.; Gordon, M. S.; Jensen, J. H.; Koseki, S.; Matsunaga, N.; Nguyen, K. A.; Su, S. J.; Windus, T. L.; Dupuis, M.; Montgomery, J. A. *J. Comput. Chem.* **1993**, *14*, 1347.
(31) Stevens, W. J.; Basch, H.; Krauss, M. *J. Chem. Phys.* **1984**, *81*, 6026.
(32) Stevens, W. J.; Krauss, M.; Basch, H.; Jasien, P. G. *Can. J. Chem.* **1992**, *70*, 612.
(33) Schäfer, A.; Horn, H.; Ahlrichs, R. *J. Chem. Phys.* **1992**, *97*, 2571.
(34) (a) Hehre, W. J.; Ditchfield, R.; Pople, J. A. *J. Chem. Phys.* **1972**, *56*, 2257. (b) Ditchfield, R.; Hehre, W. J.; Pople, J. A. *J. Chem. Phys.* **1971**, *54*, 724.
(35) Gaussian 94, Revision D.2; Frisch, M. J.; Trucks, G. W.; Schlegel, H. B.; Gill, P. M. W.; Johnson, B. G.; Robb, M. A.; Cheeseman, J. R.; Keith, T.; Petersson, G. A.; Montgomery, J. A.; Raghavachari, K.; Al-Laham, M. A.; Zakrzewski, V. G.; Ortiz, J. V.; Foresman, J. B.; Cioslowski, J.; Stefanov, B. B.; Nanayakkara, A.; Challacombe, M.; Peng, C. Y.; Ayala, P. Y.; Chen, W.; Wong, M. W.; Andres, J. L.; Replogle, E. S.; Gomperts, R.; Martin, R. L.; Fox, D. J.; Binkley, J. S.; Defrees, D. J.; Baker, J.; Stewart, J. P.; Head-Gordon, M.; Gonzalez, C.; Pople, J. A., Gaussian, Inc.: Pittsburgh, PA, 1995.
(36) (a) Baerends, E. J.; Ellis, D. E.; Ros, P. *Chem. Phys.* **1973**, *2*, 41. (b) te Velde, G.; Baerends, E. J. *J. Comput. Phys.* **1992**, *99*, 84.
(37) Vosko, S. H.; Wilk, L.; Nusair, M. *Can. J. Phys.* **1980**, *58*, 1200.
(38) Perdew, J. P.; Chevary, J. A.; Vosko, S. H.; Jackson, K. A.; Pederson, M. R.; Singh, D. J.; Fiolhais, C. *Phys. Rev. B: Condens. Matter* **1992**, *B46*, 6671.
(39) (a) Boerrigter, P. M. Ph.D. Thesis, Chemistry, Vrije Universiteit, 1987, Amsterdam. (b) Ziegler, T.; Tschinke, V.; Baerends, E. J.; Snijders, J. G.; Ravenek, W. *J. Phys. Chem.* **1989**, *93*, 3050.
(40) Cerius^2 2.0 is available from Molecular Simulations, Cambridge, UK.
(41) Åkesson, R.; Pettersson, L. G. M.; Sandström, M.; Wahlgren, U. *J. Am. Chem. Soc.* **1994**, *116*, 8691.

Table 1. Experimental Structural Parameters and Coordination Numbers of the First Hydration Shell of Al^{3+}, Ga^{3+}, and In^{3+} in Aqueous Solution

method	salt	[salt]/M	d_{ion-O}/ Å	CN	ref
X-ray	$Al(NO_3)_3$	0.5	1.90	6	44a
X-ray	$AlCl_3$	1; 2	1.90; 1.88	6	44b
X-ray	$Al(NO_3)_3$	2.53	1.87	6	44c
NMR	$Ga(ClO_4)_3$	0.67		6.0, 6.1	47a
NMR	$Ga(ClO_4)_3$			5.89−6.28	47b
NMR	$Ga(ClO_4)_3$ in water-acetone			6	47c
X-ray	$In(ClO_4)_3$	3	2.15	6	45a
X-ray	$In_2(SO_4)_3$	1.71	2.156	6 (assumed)	45b
EXAFS	$[InBr_2(H_2O)_6]^+$	1; 2; 4	2.53		48

Table 2. Calculated and Experimental M−O Bond Lengths for $[M(OH_2)_6]^{3+}$ (in Å)

	HF[a]	MP2[b]	DFT[c]	exp[d]	exp[e]
Al^{3+}	1.940	1.948	1.944	1.877	1.90[f]
Ga^{3+}	2.001	1.997	2.014	1.944	
In^{3+}	2.199	2.194	2.212	2.112	2.15, 2.156[g]

[a] GAMESS. [b] Gaussian94. [c] ADF, see computational details. [d] From the $[M(OH_2)_6]$ unit in crystalline $CsM^{III}[SO_4]_2 \cdot 12H_2O$.[43] [e] In aqueous solution. [f] At $c = 0.5$ M.[44a] [g] Reference 45.

relativistic effects), MP2 (neglecting relativistic effects), and DFT levels. The latter includes dynamic electron correlation and scalar (quasi-) relativistic corrections. The M−O bond lengths obtained by using all three levels of approximation are very similar and longer than those found in the crystal structures (Table 1). These calculations show that neither dynamic electron correlation nor relativistic effects have a pronounced effect on the geometries (Table 2). Therefore, Hartree−Fock calculations with relativistic effective core potentials are adequate for the investigation of aqua complexes of Al^{3+}, Ga^{3+}, and In^{3+}.

Dissociative Exchange Mechanism. The water-exchange reactions have been analyzed by using the previously described model[12,13] that involves seven water molecules. The reactants were represented by the water adducts of the hexahydrates. Two isomers thereof have been considered, one with the water in the second coordination sphere bound through one hydrogen bond and the other where the lattice water forms two hydrogen bonds with two water molecules form the first coordination sphere (Table 3 and Figure 1). The former structure has been used to describe the reactions of the di- and trivalent first row transition metals.[12,13] The other structure, involving two hydrogen bonds, is slightly more stable. A summary of all the M−O bond lengths is given in Table 3. As observed previously,[12] the M−O bonds carrying a hydrogen bonded water molecule in the second coordination sphere are shorter.

For all three main group ions, transition states and intermediates as well have been obtained for this pathway. The structures (Figure 1) are similar to those found for the first row transition metals.[12,13] The M−O bond lengths are listed in Table 3, and the activation energies ($\Delta E^{\ddagger}$), together with experimental data wherever available, are reported in Table 4. Figure 2a shows the energy profile relative to the linear hydrogen bond for the dissociative pathway. It can be seen that the energy difference between intermediate and its corresponding transition state ($\Delta E^{\ddagger}$) is relatively large for Al^{3+} and Ga^{3+}, but smaller for In^{3+} (Figure 2, Table 4).

Associative Exchange Mechanism. The computation of the pertinent transition states and their corresponding intermediates has been attempted for Al^{3+}, Ga^{3+}, and In^{3+}. The calculations were, however, only successful for In^{3+}. The M−O bond of the water in the second coordination sphere was shortened progressively and kept constant while all the other internal coordinates were optimized. For Al^{3+} and Ga^{3+}, this always led to pentacoordinated species, intermediates with two water molecules in the second coordination sphere (Figure 3, species **4a** and **4b** in Table 3). They arose from the simultaneous elimination of two water molecules from the first coordination sphere. For In^{3+}, the transition state together with its corresponding heptacoordinated intermediate were obtained readily (Figure 1, Table 3). These structures are the same as those found for $Sc(OH_2)_7^{3+}$, $Ti(OH_2)_7^{3+}$, $V(OH_2)_7^{3+}$, $Mn(OH_2)_7^{2+}$, $Fe(OH_2)_7^{3+}$, and $Co(OH_2)_7^{2+}$.[12,13] As Figure 2 shows, the associative pathway requires a much lower activation energy than the dissociative one, and therefore In^{3+} is very unlikely to undergo a dissociative water exchange. This contrasts the preference of Al^{3+} and Ga^{3+}, for which neither an I_a nor an A mechanism could be computed based on the present model.

Activation volume $\Delta V^{\ddagger}$. The activation volumes for water exchange on Al^{3+} and Ga^{3+} have been determined from variable-pressure NMR experiments (Table 4). The positive volumes found established a dissociatively activated reaction

Table 3. Selected Properties of Reactants/Products, Transition States, and Intermediates

species	figure	description	symmetry	energy, au	energy, kJ mol^{-1}	d(M−O), Å
$[Al(OH_2)_6 \cdot OH_2]^{3+}$		linear hydrogen bond	C_s	−533.261 823	0.00	1.88, 1.94, 1.95, 1.95, 1.95, 1.95, **3.97**
$[Al(OH_2)_6 \cdot OH_2]^{3+}$		bifurcated hydrogen bond	C_s	−533.263 267	−3.79	1.92, 1.92, 1.95, 1.95, 1.95, 1.95, **3.72**
$\{[Al(OH_2)_5 \cdots OH_2 \cdot OH_2]^{3+}\}^{\ddagger}$		dissociative transition state	C_s	−533.229 311	+85.4	1.86, 1.87, 1.89, 1.92, 1.92, **3.16**, **3.98**
$[Al(OH_2)_5 \cdot (OH_2)_2]^{3+}$		pentacoordinated intermediate	C_{2v}	−533.233 378	+74.7	1.85, 1.85, 1.89, 1.94, 1.94, **3.91**, **3.91**
$[Ga(OH_2)_6 \cdot OH_2]^{3+}$	1	linear hydrogen bond	C_s	−788.397 017	0.00	1.93, 2.00, 2.01, 2.01, 2.01, 2.02, **4.01**
$[Ga(OH_2)_6 \cdot OH_2]^{3+}$	1	bifurcated hydrogen bond	C_s	−788.399 060	−5.36	1.97, 1.97, 2.01, 2.01, 2.01, 2.02, **3.76**
$\{[Ga(OH_2)_5 \cdots OH_2 \cdot OH_2]^{3+}\}^{\ddagger}$	1	dissociative transition state	C_s	−788.370 709	+69.1	1.89, 1.92, 1.95, 2.00, 2.00, **3.11**, **4.01**
$[Ga(OH_2)_5 \cdot (OH_2)_2]^{3+}$	1	pentacoordinated intermediate	C_{2v}	−788.376 225	+54.6	1.88, 1.88, 1.94, 2.02, 2.02, **3.93**, **3.93**
$[Ga(OH_2)_5 \cdot (OH_2)_2]^{3+}$	4a	water adduct	C_{2v}[a]	−788.390 451	+17.2	1.89, 1.94, 1.94, 1.97, 1.97, **3.70**, **3.70**
$[Ga(OH_2)_5 \cdot (OH_2)_2]^{3+}$	4b	water adduct	C_2[b]	−788.393 079	+10.3	1.91, 1.91, 1.95, 1.97, 1.97, **3.73**, **3.73**
$\{[Ga(OH_2)_7]^{3+}\}^{a,c}$		hyper saddle point	C_{2v}	−788.358 030	+102	1.97, 1.97, 2.05, 2.05, 2.14, 2.28, 2.28
$[In(OH_2)_6 \cdot OH_2]^{3+}$	3	linear hydrogen bond	C_s	−719.504 081	0.00	2.13, 2.20, 2.21, 2.21, 2.21, 2.21, **4.20**
$[In(OH_2)_6 \cdot OH_2]^{3+}$	3	bifurcated hydrogen bond	C_s	−719.508 123	−10.6	2.17, 2.17, 2.21, 2.21, 2.21, 2.21, **3.93**
$\{[In(OH_2)_5 \cdots OH_2 \cdot OH_2]^{3+}\}^{\ddagger}$		dissociative transition state	C_s	−719.475 423	+75.2	2.10, 2.11, 2.17, 2.19, 2.19, **3.44**, **4.19**
$[In(OH_2)_5 \cdot (OH_2)_2]^{3+}$		pentacoordinated intermediate	C_{2v}	−719.477 577	+69.6	2.10, 2.10, 2.16, 2.20, 2.20, **4.12**, **4.12**
$\{[In(OH_2)_6 \cdots OH_2]^{3+}\}^{\ddagger}$	3	associative transition state	C_1	−719.492 991	+29.1	2.18, 2.19, 2.20, 2.23, 2.24, 2.26, **2.78**
$[In(OH_2)_7]^{3+}$	3	heptacoordinated intermediate	C_2	−719.496 593	+19.7	2.21, 2.21, 2.27, 2.28, 2.28, 2.29, 2.29
$\{[In(OH_2)_6 \cdots OH_2]^{3+}\}^{c}$		hyper saddle point	C_{2v}	−719.491 060	+34.2	2.18, 2.18, 2.20, 2.20, 2.28, 2.28, **2.83**

[a] Computed with C_2 symmetry. [b] Computed with C_1 symmetry. [c] Two imaginary frequencies.

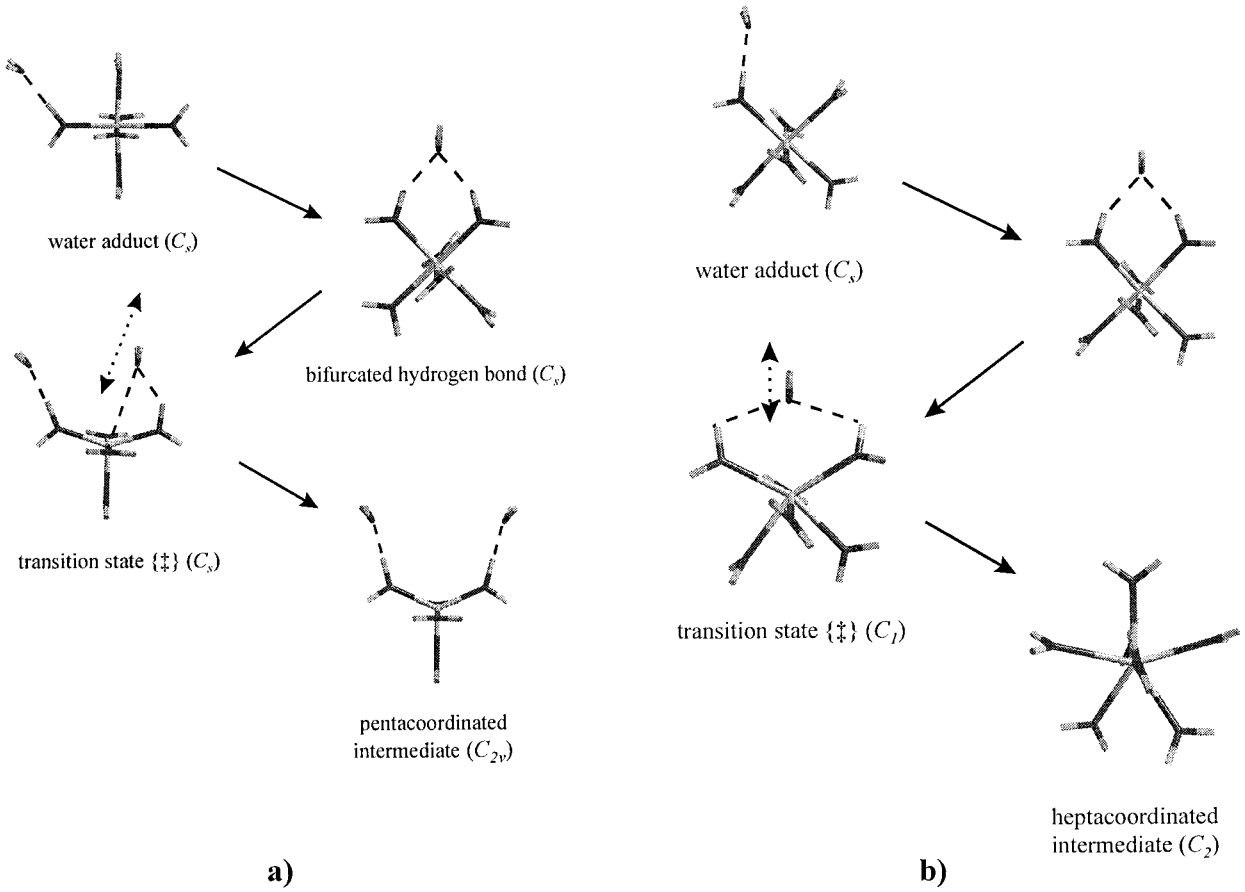

Figure 1. (a) Dissociative exchange pathway via a stable pentacoordinated aqua complex $[M(OH_2)_5{\cdot}(OH_2)_2]^{3+}$ for M = Ga^{3+}. The broken arrow shows the imaginary mode in the transition state $\{[M(OH_2)_5{\cdots}OH_2{\cdot}OH_2]^{3+}\}^{‡}$. (b) Associative exchange pathway via a stable heptacoordinated aqua complex $[M(OH_2)_7]^{3+}$ for M = In^{3+}. The broken arrow shows the imaginary mode in the transition state $\{[In(OH_2)_6{\cdots}OH_2]^{3+}\}^{‡}$.

Table 4. Experimental and Calculated Activation Parameters

	experimental				calculated		
species	$\Delta H^{‡}$, kJ mol^{-1}	$\Delta S^{‡}$, J K^{-1} mol^{-1}	$\Delta G^{‡}_{298}$, kJ mol^{-1}	$\Delta V^{‡}$, cm^3 mol^{-1}	$\Delta E^{‡}$,[a] kJ mol^{-1}	$\Delta E_I^{‡}$,[b] kJ mol^{-1}	$\Delta V^{‡}_c$ or ΔV_c,[c] cm^3 mol^{-1}
$[Al(OH_2)_6{\cdot}OH_2]^{3+}$							
$\{[Al(OH_2)_5{\cdots}OH_2{\cdot}OH_2]^{3+}\}^{‡}$	84.7[d]	+41.6[d]	72.3	+5.7[d]	+85.4	10.7	+5.6
$[Al(OH_2)_5{\cdot}(OH_2)_2]^{3+}$					+74.7		+7.1
$[Ga(OH_2)_6{\cdot}OH_2]^{3+}$							
$\{[Ga(OH_2)_5{\cdots}OH_2{\cdot}OH_2]^{3+}\}^{‡}$	67.1[e]	+30.1[e]	58.1	+5.0[e]	+69.1	14.5	+4.8
$[Ga(OH_2)_5{\cdot}(OH_2)_2]^{3+}$					+54.6		+6.9
$[In(OH_2)_6{\cdot}OH_2]^{3+}$							
$\{[In(OH_2)_5{\cdots}OH_2{\cdot}OH_2]^{3+}\}^{‡}$					+75.2	5.6	+4.4
$[In(OH_2)_5{\cdot}(OH_2)_2]^{3+}$					+69.6		+4.9
$\{[In(OH_2)_6{\cdots}OH_2]^{3+}\}^{‡}$					+29.1	9.4	−5.2
$[In(OH_2)_7]^{3+}$					+19.7		−7.1

[a] Difference in energy between transition state and linear hydrogen bond water adduct. [b] Difference in energy between transition state and penta- or heptacoordinated intermediate. [c] Difference in Connolly volume of transition state or intermediate relative to linear hydrogen bond water adduct. [d] Reference 17. [e] Reference 19.

mechanism that was assigned as I_d. To calculate activation volumes, that is the volume difference between the transition state and the ground state of the reactants, we used the Connolly surface[42] of the calculated aqua clusters. In an empirical approach we neglected the volume of the hydrogen atoms and scaled up the van der Waals radius of the water oxygen by a factor of 1.254 to reproduce the experimental $\Delta V^{‡}$ for Al^{3+} and Ga^{3+} (Table 4). Calculating the corresponding activation volumes for the dissociative and associative exchange process for In^{3+} leads to +4.4 and −5.2 cm^3 mol^{-1}, respectively. Using the same method we also computed the volumes of the penta- and heptacoordinated intermediates. In all cases this leads to a further expansion (dissociative mechanism) or retraction (associative mechanism) of the aqua cluster. Figure 4 shows volume profiles for dissociative water exchange at Al^{3+}, Ga^{3+}, and In^{3+}, and for associative water exchange at In^{3+}.

Water Exchange at In^{3+}. Unfortunately, the water exchange rate at In^{3+} was too fast to be measured, and thus precluded the measurement of a volume of activation. Equation 2 allows the determination of the rate of water exchange at a diamagnetic site, k_{dia}, in the presence of a paramagnetic (Tb^{3+}) shift reagent exchanging with a rate, k_{Tb}.[21] The difference in the ^{17}O relaxation rates of water in the presence of Tb^{3+} and a

(42) Connolly, M. L. *Science* **1983**, *221*, 709.

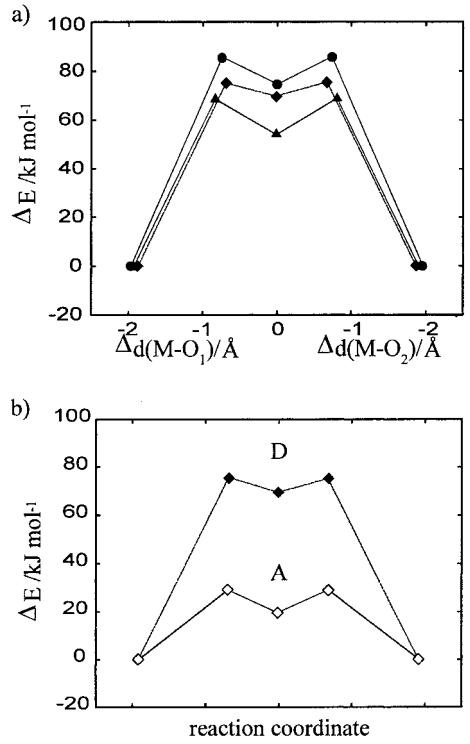

Figure 2. Energy profiles relative to the linear hydrogen bond water adduct: (a) for a dissociative D water exchange reaction on Al^{3+}(●), Ga^{3+}(▲), and In^{3+}(◆). Δ*d* is the metal−oxygen distance of the leaving or entering water molecule with respect to the distance in the pentacoordinated intermediate; (b) for an associative A (◇) and dissociative D (◆) water exchange reaction on In^{3+}.

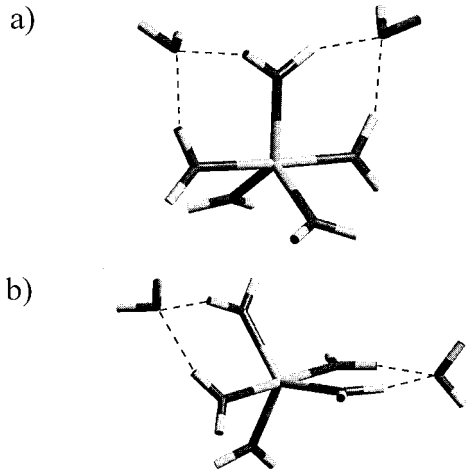

Figure 3. Pentacoordinated aqua complexes with two water molecules attached *via* bifurcated hydrogen bonds are the stable products when trying to optimize a 7-fold coordinated Ga^{3+} aqua cluster.

diamagnetic is a function of two terms, and is dependent on p_{Tb} and p_{dia}, the mole fractions of water bound to Tb^{3+} and the diamagnetic species, $\Delta\omega$, the chemical shift of water in the presence of Tb^{3+} relative to pure water, and the water exchange rates for both Tb^{3+} and the diamagnetic. The first term describes the broadening of the free water signal because of fast exchange of water molecules from the Tb^{3+} aqua ion. The second term gives the broadening due to the diamagnetic species.

$$\frac{1}{p_{Tb}}\left(\frac{1}{T_2}-\frac{1}{T_1}\right)=\left(\frac{\Delta\omega_{Tb}{}^2}{k_{Tb}}\right)+\left(\frac{p_{dia}}{p_{Tb}}\frac{k_{dia}(p_{Tb}\Delta\omega_{Tb})^2}{k_{dia}^2+(p_{Tb}\Delta\omega_{Tb})^2}\right) \quad (2)$$

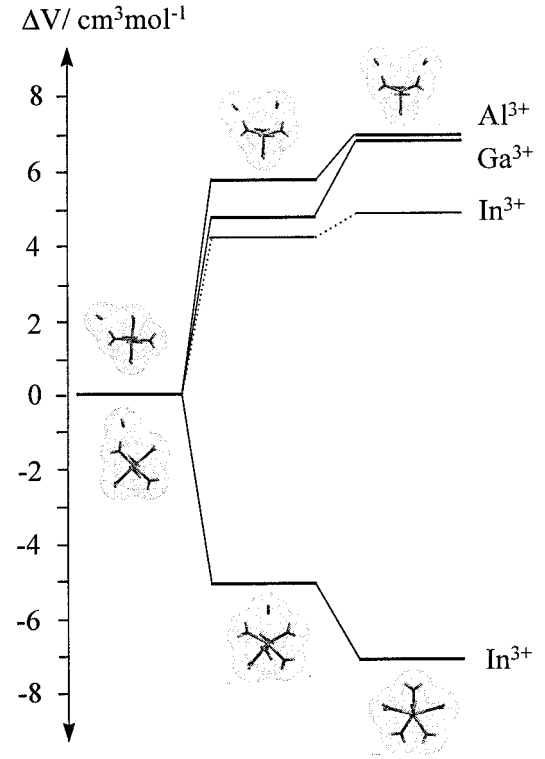

Figure 4. Volume change (reactants − transition states − intermediates) for a dissociative D water exchange (top) and an associative A water exchange (bottom).

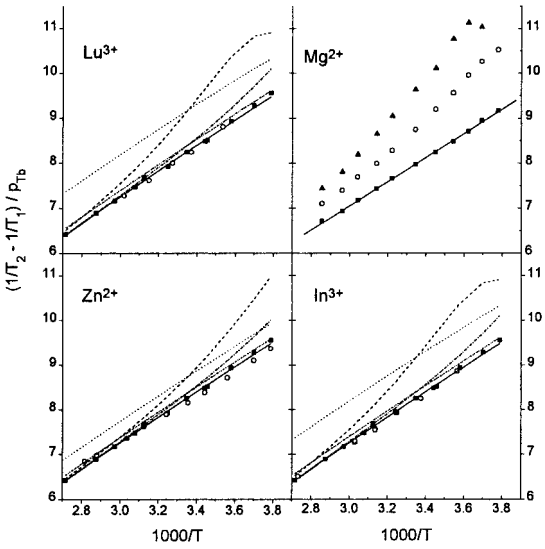

Figure 5. Experimental (points) and simulated (lines) effect of added diamagnetic ions to the ^{17}O relaxation rates of $Tb^{3+}_{(aq)}$ vs reciprocal temperature. Top left: Lu^{3+}. Top right: Mg^{2+}. Bottom left: Zn^{2+}. Bottom right: In^{3+}. See Table 5 for details.

Figure 5 shows the experimental results for Tb^{3+} alone and in the presence of In^{3+}, Lu^{3+}, Zn^{2+}, and Mg^{2+}. By dividing the relaxation rate difference by the mole fraction of terbium (left-hand side of eq 2), all results are normalized to a uniform terbium concentration. The solid squares and solid lines in each of the four plots represent the effect due to terbium alone (the first term in the right-hand side of eq 2). Thus any positive deviation from this line will be due to exchange at the diamagnetic ion. The data from the $In^{3+} + Tb^{3+}$ solution (open circles, see Table 5 for details) lie on the same line as the Tb^{3+} only data, indicating that the second term in eq 2 is negligible.

Table 5. Solution Composition and Parameters Used for Simulated Curves in Figure 5

solution composition	symbol	···, $\Delta H^{\ddagger}$, k_{298}[a]	—••—, $\Delta H^{\ddagger}$, k_{298}[a]	— —, $\Delta H^{\ddagger}$, k_{298}[a]	—•—, $\Delta H^{\ddagger}$, k_{298}[a]
Tb^{3+}(0.36 M) + In^{3+}(0.48 M)	○	15, 1×10^6	15, 1×10^7	50, 1×10^6	50, 1×10^7
Tb^{3+}(0.63 M) + Lu^{3+}(0.54 M)	○	15, 1×10^6	15, 1×10^7	50, 1×10^6	50, 1×10^7
Tb^{3+}(0.36 M) + Zn^{2+}(1.86 M)	○	15, 1×10^7	15, 5×10^7	50, 1×10^7	50, 5×10^7

[a] $\Delta H^{\ddagger}$ and k_{298} in units of kJ mol^{-1} and s^{-1} respectively, simulated curves were obtained with $p_{Tb} = 0.05$, $p_{In} = 0.05$, $p_{Lu} = 0.05$, and $p_{Zn} = 0.20$. Solid line is fit to Tb-only data, ■ for Tb only solutions (0.2−0.4 *m*). Mg^{2+} solution composition: ▲ 0.44 *m* Tb^{3+}, 0.44 *m* Mg^{2+}; ○ 0.20 *m* Tb^{3+}, 0.21 *m* Mg^{2+}. For Mg^{2+}, $k_{298} = 6.7 \times 10^5$ s^{-1} and $\Delta H^{\ddagger} = 49.1$ kJ mol^{-1}.

To estimate at what exchange rate the second term of eq 2 becomes significant, simulated curves for In^{3+} undergoing water exchange at $k_{298} = 10^6$ and 10^7 s^{-1} with enthalpies of activation of either 10 or 50 kJ mol^{-1} are also shown in Figure 5. This allows the lower limit of water exchange on In^{3+} to be increased from that reported by Glass *et al.*[20] by 3 orders of magnitude to 10^7 s^{-1}.

The magnesium results from Bleuzen *et al.*[21] are reproduced in Figure 5 to demonstrate the efficacy of this technique when measuring water exchange rates on fairly labile diamagnetic ion ($k_{298} = 6.7 \times 10^5$ s^{-1}).

As a further experimental check, Lu^{3+} was studied. The water exchange rates for the heavy lanthanide(3+) ions from Gd to Yb are known[22] and decrease across the lanthanide series. From the lanthanide results, one can estimate a rate constant for water exchange at $Lu^{3+}_{(aq)}$ of 3×10^7 s^{-1}. Figure 5 shows the experimental results of a mixed Lu^{3+}/Tb^{3+} solution. As in the case of In^{3+}, no effect was observed. Therefore the Lu^{3+} water exchange rate was greater than 10^7 s^{-1}.

It is clear from eq 2 that increasing the concentration of Tb^{3+} and/or In^{3+} should increase the observed effect. However, increasing Tb^{3+} concentrations beyond 0.7 *m* leads to severe line broadening problems and renders T_2 measurements inaccurate. Increasing In^{3+} concentrations beyond 1 *m* starts to affect the viscosity of the solution in such a way that the extreme narrowing condition (a prerequisite for eq 2) does not hold, and eq 2 becomes invalid. With the dipositive ion $Zn^{2+}_{(aq)}$, one is able to achieve higher concentrations without adverse viscosity effects. Indeed, with $Zn^{2+}_{(aq)}$ concentrations up to 2 *m* and a $Tb^{3+}_{(aq)}$ concentration of 0.5 *m* no increase in line broadening due to the diamagnetic zinc ion could be observed. This sets a lower limit of water exchange at $Zn^{2+}_{(aq)}$ at 5×10^7 s^{-1}.

Discussion

Hydration of Group 13 Aquaions. Al^{3+}, Ga^{3+}, and In^{3+} form octahedral $[M(OH_2)_6]^{3+}$ subunits in the solid cesium alums $CsM^{III}[SO_4]_2 \cdot 12H_2O$.[43] In aqueous solution coordination numbers are also 6 as revealed by X-ray diffraction for Al(III)[44] and In(III),[45] and by NMR measurements for Al(III),[45,46] Ga(III),[45,47] and In(III)[45] (see Table 1). At high salt concentration there is some evidence that In^{3+} tends to coordinate counteranions and to increase its coordination number over six. A species, $[InBr_2(H_2O)_6]^+$, has been postulated in a concentration range from 1 to 4 M from EXAFS results.[48] Isolated In^{3+} aqua ions are supposed to be present at lower bromide concentration (0.5 M).

Published theoretical studies of the hydration of Al^{3+}, Ga^{3+}, or In^{3+} are rather scarce. The geometries of the hexaaqua complexes of Ga^{3+} and In^{3+} from quantum-mechanical optimizations at the SCF level have been reported.[41] Åkesson *et al.*[41] have obtained the geometries of the pentaaqua and heptaaqua clusters of Ga^{3+} from highly constrained geometry optimizations and have proposed a dissociative interchange I_d mechanism for water exchange on $[Ga(OH_2)_6]^{3+}$. The species $[Al(OH_2)_7]^{3+}$ described by Probst and Hermannson[49] was likewise the result of a constrained optimization. To our knowledge MD simulations of aqueous solutions of Al^{3+}, Ga^{3+}, or In^{3+} are limited to a recent study of Al^{3+}, which includes interaction potential from first principles calculations.[50] The simulated results are in good agreement with the experimental value for the enthalpy of solvation and for the Al−O and Al−H radial distribution functions. However, the exchange rate is too slow to be followed in these simulations. Special simulation techniques are required to estimate exchange rate constants and activation parameters from MD simulations with reasonable computational effort.[51]

Attribution of the Exchange Mechanism. For the di- and trivalent first row transition metal aqua ions, pathways corresponding to the A, I_a, and D mechanisms have been inferred from model computations.[12,13] The present calculations provided the same type of structures. The D mechanism is feasible for Al^{3+}, Ga^{3+}, and In^{3+}, whereas the A mechanism applies, at least within the present model, only for In^{3+}, for which it is even the most favorable pathway. Hence, In^{3+} is predicted to undergo water-exchange via the A mechanism in contrast to Al^{3+} and Ga^{3+} for which is was impossible to obtain transition states corresponding to the A or I_a mechanisms.

As pointed out in other work,[13] the distinction between A and I_a or D and I_d mechanisms might under certain circumstances depend on the model, for instance, the treatment of the second coordination sphere and the bulk. For the presently investigated systems, the $\Delta E_I^{\ddagger}$ values, describing the stability of the intermediates, are relatively large (>10 kJ/mol). Therefore, improvements of the model are unlikely to change the energies of the transition state and corresponding intermediate in such a way that the energy of the latter becomes higher than that of the transition state. In that situation, the A or D mechanisms respectively would become I_a or I_d.

In Table 4, the experimental heats of activation, $\Delta H^{\ddagger}$, for water exchange at the group 13 metal aqua ions are given along with the values calculated as described above. The excellent

(43) Beattie, J. K.; Best, S. P.; Skelton, B. W.; White, A. H. *J. Chem. Soc., Dalton* **1981**, 2105.
(44) (a) Bol, W.; Welzen, T. *Chem. Phys. Lett.* **1977**, *49*, 189. (b) Caminiti, R.; Licheri, G.; Piccaluga, G.; Pinna, G.; Radnai, T. *J. Chem. Phys.* **1979**, *71*, 2473. (c) Caminiti, R.; Radnai, T. *Z. Naturforsch.* **1980**, *35a*, 1368.
(45) (a) Maeda, M.; Ohtaki, H. *Bull. Chem. Soc. Jpn.* **1977**, *50*, 1893. (b) Caminiti, R.; Paschina, G. *Chem. Phys. Lett*. **1981**, *82*, 487. (c) Fratiello, A.; Lee, R. E.; Nishida, V. M.; Schuster, R. E., *J. Chem. Phys.* **1968**, *48*, 3705.
(46) (a) Connick, R. E.; Fiat, D. N. *J. Chem. Phys.* **1963**, *39*, 1349. (b) Alei, M.; Jackson, J. A. *J. Chem. Phys.* **1964**, *41*, 3402.
(47) (a) Swift, T. J.; Fritz, O. G.; Stephenson, F. A. *J. Chem. Phys*. **1967**, *46*, 406. (b) Fiat, D.; Connick, R. E. *J. Am. Chem. Soc*. **1966**, *88*, 4754. (c) Fratiello, A.; Lee, R. E.; Schuster, R. E. *Inorg. Chem*. **1970**, *9*, 82.
(48) de Barros Marques, M. I.; Lagarde, P. *J. Phys.: Condens. Matter* **1990**, *2*, 231.
(49) Probst, M. M.; Hermansson, K. J. *J. Chem. Phys.* **1992**, *96*, 8995.
(50) Wasserman, E.; Rustad, J. R.; Xantheas, S. S. *J. Chem. Phys*. **1997**, *106*, 9769.
(51) Rey, R.; Hynes, J. T. *J. Phys. Chem*. **1996**, *100*, 5611.

Table 6. Experimental Kinetic Parameters[a] for Solvent Exchange on Al^{3+}, Ga^{3+}, Sc^{3+}, and In^{3+} in d_3-Nitromethane Diluent (Calculated Values Are reported in Parentheses)

$[M(solvent)_6]^{3+}$	r, Å	k_{298}[a,b]	$\Delta G_{298}^{\ddagger}$, kJ mol^{-1}	$\Delta H^{\ddagger}$, kJ mol^{-1}	$\Delta S^{\ddagger}$, kJ mol^{-1}	$\Delta V^{\ddagger}$, cm^3 mol^{-1}	mechanism
$Al(H_2O)_6^{3+}$	0.53	1.29[b]	72.3	84.7 (85.4)	+41.6	+5.7 (+5.6)	D
$Al(DMSO)_6^{3+}$		0.30[c]	76.0	82.6	+22.3	+15.6	D
$Al(DMF)_6^{3+}$		0.05[c]	79.8	88.3	+28.4	+13.7	D
$Al(TMP)_6^{3+}$		0.78[c]	73.7	85.1	+38.2	+22.5	D
$Ga(H_2O)_6^{3+}$	0.62	403[b]	58.1	67.1 (69.1)	+30.1	+5.0 (+4.8)	D
$Ga(DMSO)_6^{3+}$		1.87[c]	71.5	72.5	+3.5	+13.1	D
$Ga(DMF)_6^{3+}$		1.72[c]	71.7	85.1	+45.1	+7.9	D
$Ga(TMP)_6^{3+}$		6.4[c]	68.5	76.5	+27.0	+20.7	D
$Sc(TMP)_6^{3+}$	0.75	39[d]	64.0	21.2	−143.5	−18.7	A, I_a
$Sc(TMP)_6^{3+}$ c		139[e]	55.4	37.4	−60.5	−20.1	A, I_a
$In(H_2O)_6^{3+}$	0.80	$\geq 1 \times 10^7$	$\leq$33.1	? (29.1)	?	? (−5.2)	A
$In(TMP)_6^{3+}$		7.6[d]	68.0	32.8	−118	−22.8	A, I_a

[a] Values taken from ref 3. [b] In neat water, first order rate constant (k_1/s^{-1}). [c] First order rate law (k_1/s^{-1}). [d] Second order rate law (k_2/m^{-1} s^{-1}). [e] By ^{45}Sc NMR in neat TMP, second order rate constant (k_2/m^{-1} s^{-1}), ref 57.

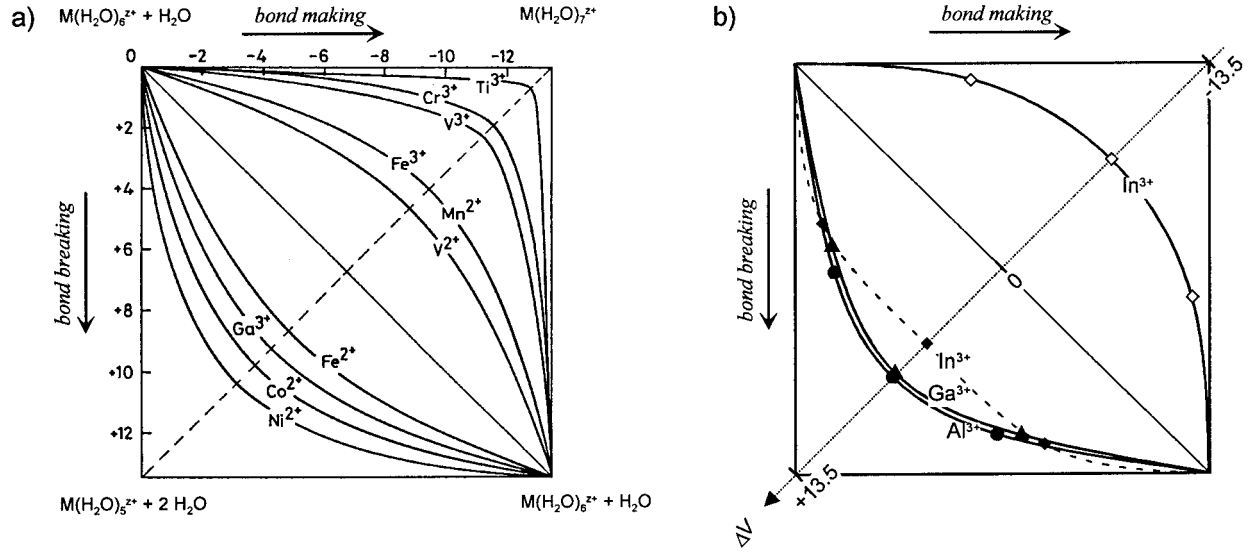

Figure 6. Interpretation of volumes of activation for water exchange on aqueous $M(H_2O)_6^{z+}$ in terms of contributions (cm^3 mol^{-1}) from bond making and bond breaking: (a) summary of volumes of activation for metal aqua ions,[3] (b) calculated curves for Al(III), Ga(III), and In(III) with use of the Connolly volumes in Table 4.

agreement between the calculated and experimental values for $Al^{3+}_{(aq)}$ and $Ga^{3+}_{(aq)}$ gives confidence to the model employed here. On the basis of this model, the mechanisms for water exchange at Al^{3+} and Ga^{3+} are both proposed to be D. Likewise, the much lower energy pathway for an **a** activated mechanism for $In^{3+}_{(aq)}$ coupled with the presence of a stable seven coordinate intermediate allows the mechanism for water exchange at $In^{3+}_{(aq)}$ to be assigned as A.

Al^{3+}, Ga^{3+}, Sc^{3+}, In^{3+} in organic solvents. The substitution behavior of the d^{10} group 13 metal ions and their d^0 group 3 analogue, Sc^{3+}, in organic solvents is fairly well established. The addition of an inert diluent, such as nitromethane, allows direct access to the rate law, something which cannot be obtained in aqueous media. Studies have been carried out on Al(III) and Ga(III) solvates of DMF, DMSO, and TMP and on the Sc(III) and In(III) TMPA complexes[52] and are summarized in Table 6. As the size of the metal center increases from Al to Ga to In, the solvent lability also increases. Concurrent with this increase in lability, the volume of activation is positive for Al(III), slightly smaller for Ga(III), and negative for Sc(III) and In(III), suggesting a crossover in mechanism from **d** to **a** activation between Ga(III) and Sc(III). The change in mechanistic behavior is also reflected in the enthalpies and entropies of activation. $\Delta H^{\ddagger}$ decreases down the group and $\Delta S^{\ddagger}$ changes from positive to negative, again suggesting a change in mechanism. The order of the reactions is also consistent with a mechanistic crossover. The **d** activated Al^{3+} and Ga^{3+} substitutions are first-order reactions while the **a** activated Sc^{3+} and In^{3+} substitutions are second-order reactions. The smaller Al^{3+} and Ga^{3+} are clearly exchanging via a D mechanism, while for Sc^{3+} and In^{3+} an A mechanism is likely operating, but an I_a mechanism cannot be ruled out.

Relation between Mechanism and Activation Volume. Swaddle has scaled a More-O'Ferrall diagram (a square whose sides represent M−X and M−Y bond order changes from 0 to 1 for a reaction $ML_nX + Y \rightarrow ML_nY + X$)[2] to the physical parameter volume. This can be done by scaling the diagram with a semiempirical description of the partial molar volume of a metal ion for a symmetrical water exchange reaction,[3] Figure 6a. The problem with attaching physical reality to such a system is that only one point is measurable, $\Delta V^{\ddagger}$ the volume change from ground state to transition state. This volume will ultimately consist of contributions from bond making and bond

(52) Values for the nonaqueous solvent exchange taken from ref 3. DMF = *N*,*N*′-dimethylformamide, DMSO = dimethyl sulfoxide, TMP = trimethyl phosphate.

breaking, the *x* and *y* coordinates, and it is not obvious where on this two-dimensional space to place the measured volume. Swaddle has argued[53] that all water exchange reactions should be regarded as having interchange, I, mechanisms, which span a continuum in which the degree of bond making by the incoming solvent molecule ranges from very substantial to negligible. For an interchange mechanism, the transition state would necessarily lie on the dashed diagonal in Figure 6a. Taking this approach, the measured volume of activation can be placed on the diagonal at such a point where cancellation of positive volume for bond breaking with negative volume for bond making gives the measured volume, e.g. the measured $\Delta V^{\ddagger}$ for water exchange at $Fe^{3+}_{(aq)}$ is -5.4 cm^3 mol^{-1} which would be placed on the diagonal at -9.4 and $+4.0$. It should be stressed that in this model the A and D mechanisms are considered as the limiting cases for the interchange mechanistic continuum and are therefore following the edges of the square diagram with "transition states/intermediates" located at the corners of the square diagram.

In cases where intermediates for solvent exchange reactions have been identified (contrarly to the interchange postulate of Swaddle) a different view of the square diagram has to be defined. In Figure 6b we have kept the empirical limits of ± 13.5 cm^3 mol^{-1}, since this choice allows us to compare stepwise (A and D) and concerted (I) mechanisms on the same diagram. For concerted mechanisms I, the single transition state lies as before on the ΔV axes diagonal. However, for stepwise mechanisms, the intermediate lies on the diagonal (and not necessarily on a corner), while the two symmetric transition states lie symmetrically off to the diagonal. The computed structures and volume changes for Al^{3+}, Ga^{3+}, and In^{3+} water exchange can be used to introduce the position of transition states and intermediates in our diagram (Figure 6b) with use of the following definitions: (i) the M−O bond length for the dissociative limit d_{max} is equal to the M···O distance of the water in the second coordination sphere of $[M(OH_2)_6 \cdot OH_2]^{n+}$; (ii) the "normal" M−O bond length d_{normal} is the average of the six M−O bonds of $[M(OH_2)_6 \cdot OH_2]^{n+}$; (iii) for the transition state the M···O bond length is labeled $d_{A,TS}$ or $d_{D,TS}$; (iv) the (normal) M−O bonds in the transition state for the A and D mechanisms are called $d_{A,M-O}$, and $d_{D,M-O}$, respectively; and (v) the parameters d_{form} and d_{break} for bond formation and breaking, respectively, in the transition state are defined for the D and A mechanism by eqs 3 and 4.

$$\text{D:} \quad d_{break} = d_{D,TS} - d_{normal} \tag{3}$$

$$d_{form} = \sum_{i=1}^{5} (d_{normal} - d_{i,D,M-O})$$

$$\text{A:} \quad d_{break} = \sum_{i=1}^{6} (d_{i,A,M-O} - d_{normal}) \tag{4}$$

$$d_{form} = d_{max} - d_{A,TS}$$

Calculated ΔV_C or $\Delta V^{\ddagger}_C$ values (Table 4) depend on three factors, namely the magnitude of the normal M−O bonds, the degree of bond formation or breaking (expressed by d_{form} or d_{break}) and the M···O bond length $d_{A,TS}$ or $d_{D,TS}$ in the transition state. Figure 6b shows that the transition states are, as pointed out earlier,[12] about half the way between the reactant and the intermediate. This is the reason for the nonconcerted A or D mechanism, the volume of activation can be quite far away from the limiting values[54] of -13.5 or $+13.5$ cm^3 mol^{-1}, respectively. It is interesting to note that the unfavorable dissociative reaction of In^{3+} gives rise to a quite ill-behaved reaction pathway (Figure 6b).

Water Exchange on In^{3+}, Lu^{3+}, and Zn^{2+}. It was disappointing not to be able to measure water exchange rates, and hence a volume of activation, at $In^{3+}_{(aq)}$ in order to verify our postulated **a** activated mechanism. However, the current experimental study shows that older estimates of water exchange for In^{3+} and Zn^{2+} are too low. Despite stating that their value for water exchange at In^{3+} was a lower limit, the value quoted by Glass *et al.*[20] has been incorporated into tables of water exchange listed in reviews and text books. This work has succeeded in defining a lower limit for In^{3+} that is 3 orders of magnitude faster than the old value. Extrapolation of the water exchange rates on the heavy lanthanide(III) aquaions[22] leads to an estimated water exchange rate for Lu^{3+} of 3×10^7 s^{-1}. This value is just beyond the reach of the NMR method employed in this article, and the lower limit of 1×10^7 s^{-1} is in agreement with this estimate. For Zn^{2+}, ultrasonic relaxation data obtained from substitution by various ligands,[55] if interpreted in an Eigen−Wilkins manner, would be suggestive of $k \sim 3 \times 10^7$ s^{-1}. The lower limit of 5×10^7 s^{-1} determined here extends this limiting value of Eigen.

Conclusions. Within the limits of our computational model, we have shown an alternate view of the interpretation of $\Delta V^{\ddagger}$ for water substitution mechanisms. For a symmetrical reaction involving an intermediate (**A** or **D**), the intermediate should lie approximately halfway between reactants and products, along the diagonal in the More-O'Ferral type square diagram. The volume of activation corresponds to a transition state that does not lie on this diagonal. Thus, for true **A** or **D** mechanisms, the magnitude of the volume of activation will be less than some so-called limiting value. For a concerted reaction, the magnitude of the volume of activation would determine the amount of **a** or **d** character the interchange has. The results of our modeling studies suggest that the mechanisms of solvent exchange at $Al^{3+}_{(aq)}$, $Ga^{3+}_{(aq)}$, and $In^{3+}_{(aq)}$ are D, D, and A, respectively. Experimentally the detection of intermediates should prove elusive. It is in better computer modeling that the answer lies.

Acknowledgment. P.C. would like to thank the Natural Sciences and Engineering Research Council of Canada for a postdoctoral fellowship (1997−99). We wish to thank Professor Dr. M. W. Schmidt for a copy of the GAMESS program package. We are grateful to the Centro Svizzero di Calcolo Scientifico (CSCS) for CPU time on their HP 9000/735 cluster. This work was financially supported by the Swiss National Science Foundation (Grant No. 20-52630.97) and the Swiss OFES as part of the European COST D3 action.

JA980571F

(53) Swaddle, T. W. *Comments Inorg. Chem.* **1991**, *12*, 237.
(54) Swaddle, T. W. *Inorg. Chem.*, **1983**, *22*, 2663.
(55) Eigen, M. *Pure Appl. Chem.* **1963**, *6*, 105.
(56) Richens, D. T. *The Chemistry of Aqua Ions*; Wiley: Chichester, 1997.
(57) Helm, L.; Ammann, C.; Merbach, A. E. *Z. Phys. Chem. Neue Folge* **1987**, *155*, 145.